ORIGINAL PAPER

Enhanced electrochemical properties of polyethylene oxide-based composite solid polymer electrolytes with porous inorganic–organic hybrid polyphosphazene nanotubes as fillers

Jiawei Zhang · Xiaobin Huang · Hao Wei · Jianwei Fu · Yawen Huang · Xiaozhen Tang

Abstract Solid composite polymer electrolytes consisting of polyethylene oxide (PEO), LiClO$_4$, and porous inorganic–organic hybrid poly (cyclotriphosphazene-co-4, 4′-sulfonyldiphenol) (PZS) nanotubes were prepared using the solvent casting method. Differential scanning calorimetry and scanning electron microscopy were used to determine the characteristics of the composite polymer electrolytes. The ionic conductivity, lithium ion transference number, and electrochemical stability window can be enhanced after the addition of PZS nanotubes. The electrochemical impedance showed that the conductivity was improved significantly. Maximum ionic conductivity values of 1.5×10^{-5} S cm^{-1} at ambient temperature and 7.8×10^{-4} S cm^{-1} at 80 °C were obtained with 10 wt.% content of PZS nanotubes, and the lithium ion transference number was 0.35. The good electrochemical properties of the solid-state composite polymer electrolytes suggested that the porous inorganic–organic hybrid polyphosphazene nanotubes had a promising use as fillers in SPEs and the PEO$_{10}$–LiClO$_4$–PZS nanotube solid composite polymer electrolyte might be used as a candidate material for lithium polymer batteries.

Introduction

A solid polymer electrolyte (SPE) based on polyethylene oxide (PEO) is one of the promising electrolytes for high energy density secondary lithium batteries [1, 2]. Polymer electrolytes based on PEO have characteristic properties such as processability, flexibility, lightweight, elasticity, and transparency. However, the ionic conductivity of the PEO-based SPE at ambient temperature is relatively low for commercial use. Much work has been carried out to optimize the polymer electrolytes to enhance ionic conductivity, thermal stability, and electrochemical stability as the prerequisite for their use in lithium rechargeable batteries at ambient temperature. In recent years, substantial interest has been devoted to nanocomposite polymeric materials because of their superior properties such as ionic conductivity and mechanical stability over pure polymer electrolytes [3–5]. The basic method of composite polymer electrolyte (CPE) formation is the dispersion of inorganic oxides such as SiO$_2$, TiO$_2$, Al$_2$O$_3$, etc., into a polymer–salt electrolyte solid matrix [6–10]. Moreover, microporous molecular sieves such as MCM-41 and SBA-15 have been

J. Zhang · X. Huang (✉) · J. Fu · Y. Huang
School of Chemistry and Chemical Engineering,
Shanghai Jiao Tong University,
800 Dongchuan Road,
Shanghai, 200240, China
e-mail: xbhuang@sjtu.edu.cn

H. Wei
National Key Laboratory of Nano/Micro Fabrication Technology,
Key Laboratory for Thin Film and Microfabrication Technology
of Ministry of Education, Institute of Micro/Nano Science and
Technology, Shanghai Jiao Tong University,
Shanghai 200240, People's Republic of China

X. Tang
School of Chemistry and Chemical Engineering, State Key
Laboratory of Metallic Matrix Composite Material,
Shanghai Jiao Tong University,
800 Dongchuan Road,
Shanghai 200240, China

added into PEO matrix to enhance the electrochemical properties including ionic conductivity, lithium ion transference numbers, lithium electrode interface stability, and electrochemical stability markedly [11–13]. A commonly accepted formation mechanism between the filler and polymer is the complex formation through Lewis acid–base interactions [14–16]. However, inorganic ceramic fillers are not easy to aggregate into polymer electrolytes because of their poor compatibility with polymers, and the ionic conductivity and lithium ion transference numbers of the SPEs based on the ceramic fillers are usually low due to the one-dimensional topological structure of the fillers.

Hexachlorocyclotriphosphazene (HCCP) plays a crucial role in the development of new polymers because of the excellent tailoring property of the backbone and the unprecedented structural diversity [17, 18]. Recently, our group has demonstrated for the first time the preparation of novel porous uniform cyclomatrix-type polyphosphazene nanotubes via precipitation polymerization [19, 20]. It shows that HCCP possesses special potential in the fabrication of molecular-level inorganic–organic hybrid nanoscale materials. Compared with traditional ceramic fillers which are easy to aggregate when highly loaded, poly (cyclotriphosphazene-co-4, 4′-sulfonyldiphenol) (PZS) nanotubes may have better compatibility with PEO chains due to their inorganic–organic hybrid structure and to the fact that their conductivity and lithium ion transference number might be enhanced. Among nanotubes with hybrid inorganic–organic structure, PZS nanotubes might also enhance the mechanical strength of polymer electrolytes. With the above properties, PZS nanotubes may be a new class of fillers in the development of solid composite polymer electrolytes. In this paper, CPEs based on poly(ethylene oxide) with porous PZS nanotubes as fillers were prepared by using LiClO$_4$ as doping salts in order to study the effects of PZS nanotubes on performances of CPEs.

Experimental

Materials

PEO, M_w=200,000 (Shanghai Chemical Reagent Company, SCRC, Shanghai, China), and LiClO$_4$, A.R. (SCRC), were vacuum dried for 24 h at 50 °C and 120 °C, respectively. Acetonitrile, A.R. (SCRC), dehydrate by 4-A molecular sieves before use. Tetrahydrofuran (THF; SCRC) was distilled over sodium under dry nitrogen atmosphere prior to use.

HCCP (synthesized as described in the literature [21]) was recrystallized from dry hexane followed by two times sublimation. The melting point of purified HCCP was 113–114 °C. 4, 4′-Sulfonyldiphenol (BPS), triethylamine (TEA), and SiO$_2$ (average diameter 30 nm) were purchased from Shanghai Chemical Reagent Company and used without further purification.

Preparation of porous cyclomatrix-type polyphosphazene nanotubes was via an in situ template approach. The preparation of PZS nanotubes (PZSNT) was carried out as follows (Scheme 1) [20]: 50 ml THF with HCCP (0.4 g, 1.15 mmol) was added dropwise into 50 ml THF with BPS (0.86 g, 3.45 mmol) and TEA (1.04 g, 10.3 mmol) under ultrasonic irradiation (50 W, 40 Hz) at 40 °C. After ultrasonic irradiation for 24 h, the solution was filtered and then the precipitates were washed three times, respectively, with THF and deionized water. Finally, the resulting products were dried under vacuum to yield PZS nanotubes.

Preparation of CPEs

The preparation of CPEs involved first the dispersion of the fillers and LiClO$_4$ by ultrasonication in anhydrous acetonitrile at room temperature and the addition of the PEO/acetonitrile solution. The resulting slurry was cast onto a

Scheme 1 Synthetic route and chemical structure of PZS nanotubes
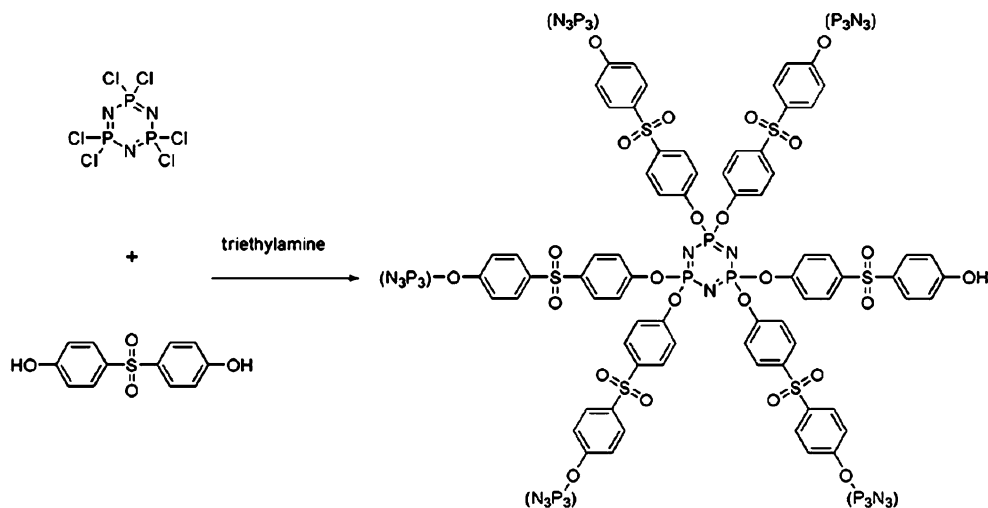
Teflon plate, and then the plate was exposed to air flow to let the solvent evaporate. Finally, the resulting films were dried under vacuum at 50 °C for 24 h to remove the residual solvent. These procedures yielded transparent homogenous films. The average thickness of the polymer electrolytes was about 100 μm. All the CPE films were stored in an argon atmosphere glove box before testing. The CPE samples used in this study were denoted as PEO_{10}–$LiClO_4$/x% filler or PEO_{10}–$LiClO_4$–x% filler, in which the EO/Li ratio was fixed to 10 for all samples and the content of filler, x, ranged from 0 to 30 wt.% of the PEO weight.

Characterization and instruments

Scanning electron microscopy (SEM) images of the surface of CPEs were observed on a JEOL JSM-7401F (JEOL Ltd., Tokyo, Japan) field emission SEM instrument with gold sputtered-coated films. CPEs films were broken in liquid nitrogen to obtain a cross-sectional SEM image.

Differential scanning calorimeter (DSC) measurements were carried out on a Perkin-Elmer Pyris-1 analyzer (PerkinElmer, Inc., Waltham, MA, USA). The measurements were carried out at a heating rate of 10 °C min^{-1} from −60 °C to 100 °C in the heating cycle and from 100 °C to −20 °C in the cooling cycle.

Ionic conductivity of the CPEs was determined by ac impedance spectroscopy. The film was sandwiched between two stainless steel (SS) blocking electrodes (with a diameter of 1 cm) to form a symmetrical SS/CPE/SS cell. The impedance tests were carried out in the 1 MHz to 1 Hz frequency range using a Solartron 1260 Impedance/Gain-Phase Analyzer (Solartron Analytical, AMETEK, Inc., Hampshire, UK) coupled with a Solartron 1287 Electrochemical Interface (Solartron Analytical, AMETEK, Inc., Hampshire, UK). The equation for calculating the conductivity is $\sigma = \frac{1}{R_p} \times \frac{d}{S}$, where d is the thickness of the polymer electrolytes and S is the area. R_p is the bulk resistance of the polymer electrolytes.

Lithium ion transference number, T_{Li^+}, was evaluated using the method of ac impedance combined with steady-state current technique, proposed by Vincent and Bruce [22–25], which involved a combination of ac and dc measurements. The method consists of initial measurement of the lithium interfacial resistance (R_0) by impedance spectroscopy in the 100-kHz–0.1-Hz frequency range, then application of a small voltage (<30 mV) until a steady current (I_{ss}) is obtained (time=3,000 s), and finally measurement of the interfacial resistance (R_{ss}) by impedance spectroscopy in the 100-kHz–0.1-Hz frequency range. According to this method, the lithium ion transference number may be calculated from the following equation:

$$T_{Li^+} = \frac{I_{ss}}{I_0}\left(\frac{\Delta V - I_0 R_0}{\Delta V - I_{ss} R_{ss}}\right)$$

where ΔV is the voltage pulse, R_0 is the initial lithium interfacial resistance, and R_{ss} is the secondary lithium interfacial resistance (as the steady-state polarization current is reached). I_0 is the initial current and I_{ss} is the current reached in the steady state. The parameters for the calculation can be obtained from the impedance response and steady-state current response. Measurements were performed using a Solartron 1260 Impedance/Gain-Phase Analyzer coupled with a Solartron 1287 Electrochemical Interface. The CPE was sandwiched between two lithium-unblocking electrodes to form a symmetrical Li/CPE/Li cell and was closed in a coin cell. The cell was assembled and sealed in an argon-filled UNILAB glove box (M. Braun Inertgas-Systeme GmbH, Garching, Germany; O_2<1 ppm; H_2O<0.1 ppm). Electrochemical stability window of the CPEs was determined by running a linear sweep voltammetry in three electrode cells using stainless steel as the blocking working electrode, lithium as both the counter and the reference electrode, and the CPE film as the electrolyte. A Solartron 1287 Electrochemical Interface was used to run the voltammetry at a scan rate of 1 mV s^{-1}.

Results and discussion

SEM image of PZS nanotubes

Figure 1 shows the SEM image of PZS nanotubes prepared by polycondensation of monomers HCCP and BPS. The products are almost uniform short nanorods with 60–80 nm in outer diameter and several micrometers in length.

Surface morphology

Scanning electron micrographs of various CPEs are displayed in Fig. 2. The micrograph for PEO_{10}–$LiClO_4$ film shows a rough surface in Fig. 2a. On blending with PZS nanotubes, the surface morphology was obviously
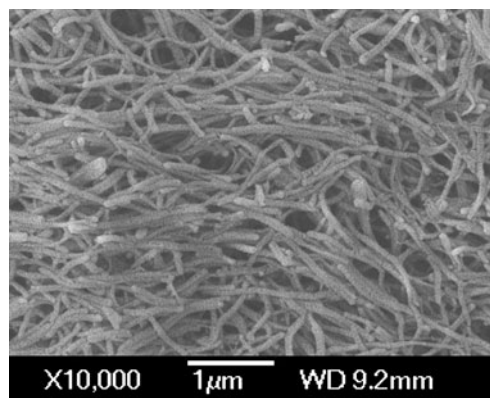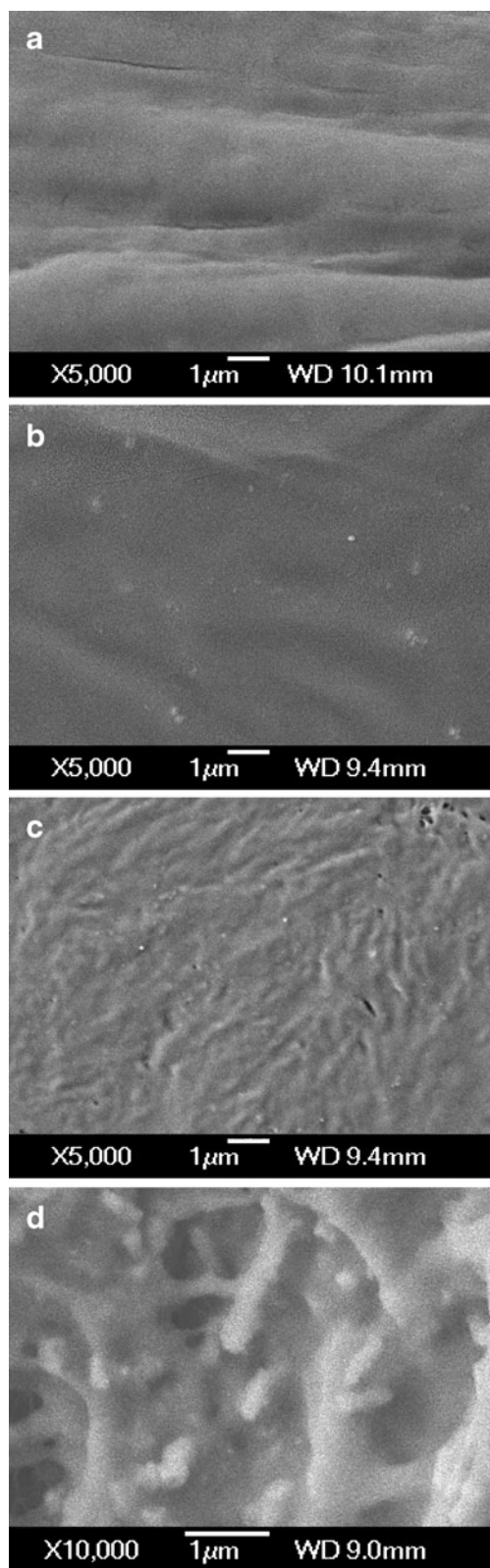

Fig. 1 SEM image of PZSNT nanotubes

Fig. 2 Surface SEM images of **a** PEO_{10}–$LiClO_4$, **b** PEO_{10}–$LiClO_4$/ 10% PZSNT, **c** PEO_{10}–$LiClO_4$/30% PZSNT composite polymer electrolytes, and **d** cross-sectional image of PEO_{10}–$LiClO_4$/10% PZSNT composite polymer electrolyte

changed from rough to smooth (Fig. 2b). The smooth morphology demonstrated that PZS nanotubes were homogeneously dispersed in the matrix of solid composite polymer electrolyte. This may be related to the reduction of PEO crystallinity upon blending with PZS nanotubes, making good compatibility between PEO polymer matrix and PZSNT. The compatibility between the polymer matrix and the fillers has great influence on the properties of the PEO-based composite polymer electrolytes. The morphology of the electrolytes only became rough when the content of PZSNT further increased (Fig. 2c), owing to the good compatibility of the filler, reducing the aggregation of PZSNT nanotubes at high loading content.

Figure 2d shows the cross-sectional image of PEO_{10}– $LiClO_4$/10% PZSNT composite polymer electrolytes. It can be seen that PZSNT can disperse homogeneously into the PEO matrix, which suggests their good compatibility. The interpenetrating network formed between PZSNT nanotubes and PEO polymer matrix may also enhance the mechanical strength of the polymer electrolytes.

Thermal analysis of composite polymer electrolytes

Detailed thermal properties of PEO_{10}–$LiClO_4$ and PEO_{10}– $LiClO_4$/x% PZSNT composite polymer electrolytes obtained from DSC analysis are summarized in Table 1. The relative percentage of crystallinity (X_c) has been calculated using the equation $X_c = (\Delta H_m^{sample} / \Delta H_m^*) \times 100$, where ΔH_m^* is the melting enthalpy of a completely crystalline PEO sample. The crystallinity value can describe the relative change of the crystalline or amorphous phase of composite electrolytes [26–28]. It can be seen from Table 1 that both the glass transition temperature (T_g) and the crystallinity of PEO (X_c) decrease obviously when PZS nanotubes are added in PEO_{10}–$LiClO_4$ complex. T_g of PEO_{10}–$LiClO_4$/x% PZSNT decreases from −34.9 °C to −46.6 °C when the content of PZS nanotubes increases from 0 to 20 wt.%. At the same time, X_c of PEO_{10}–$LiClO_4$/x% PZSNT decreases from 44.0% to 27.7%. In addition, PZS nanotubes can also decrease the melting temperature (T_m) of PEO from 60.5 °C to 54.1 °C with increasing content of PZS nanotubes.

The decrease of T_g and X_c indicates the increase of flexibility of PEO chains and the ratio of amorphous state PEO. This may be because of the good compatibility between PZSNT and PEO chains and the coordination between the ether O atoms of PEO chains and Li^+ cations. As a result, the conductivity should be enhanced at low temperatures.

Electrochemical behavior

Figure 3 shows the temperature dependence of ionic conductivity for PEO_{10}–$LiClO_4$/x% PZSNT composite

Table 1 Thermal properties of PEO$_{10}$–LiClO$_4$ and PEO$_{10}$–LiClO$_4$/x% PZSNT composite polymer electrolytes obtained from DSC analysis

Sample	Glass transition temperature T_g (°C)	Melting point T_m (°C)	Melting enthalpy[a] ΔH_m (J g^{-1})	Crystallinity[b] X_c (%)
PEO$_{10}$–LiClO$_4$	−34.9	60.5	94.0	44.0
PEO$_{10}$–LiClO$_4$/5% PZSNT	−39.4	58.1	77.6	36.3
PEO$_{10}$–LiClO$_4$/10% PZSNT	−43.9	57.0	65.2	30.5
PEO$_{10}$–LiClO$_4$/15% PZSNT	−46.4	55.5	61.5	28.8
PEO$_{10}$–LiClO$_4$/20% PZSNT	−46.6	54.1	59.2	27.7

[a] The data have been normalized to the weight of the PEO matrix

[b] $X_c = (\Delta H_m^{sample} / \Delta H_m^*) \times 100$, where $\Delta H_m^* = 213.7$ J g^{-1}

polymer electrolytes. The introduction of PZSNT had a significant effect on the ionic conductivity of CPE. The enhancement of ionic conductivity was most pronounced at low temperature. All the curves had a turning point around 50–60 °C, corresponding to the transition from the crystalline state of PEO to the amorphous phase. In the case of SPEs containing PZSNT below 60 °C, the conductivity shows a larger increase in conductivity than the SPEs above 60 °C. This result is related to the fact that the ion conductivity occurs mainly through the amorphous region of the PEO matrix [29].

As seen in Fig. 3, the conductivity increases with the increase of PZSNT content and then attains a maximum value when PZSNT concentration is about 10 wt.%. Then the conductivity decreases with further increasing PZSNT content. Decreasing the ionic conductivity was attributed to the blocking effect on the transport of charge carriers, resulting from the high loading content of the PZS nanotubes.

One reason of the enhancement in ionic conductivity with the addition of PZSNT fillers is due to the increase of the ratio of the amorphous phase of PEO and the release of more free Li$^+$. The hybrid inorganic–organic structure of PZSNT increases the ratios of the amorphous phase of PEO by lowering of the PEO reorganization, which is beneficial for the transport of Li$^+$ cations. On the other hand, the oxygen atoms, nitrogen atoms, and sulfur atoms on the surface of PZSNT coordinating with Li$^+$ cations can enhance the dissolvability of LiClO$_4$ in PEO matrix and lead to more free Li$^+$. The weakening of the polymer–cation association and Li$^+$–ClO$_4^-$ contact-ion pairs induced by PZS nanotubes may be important for ionic conduction. In the case of the solid composite polymer electrolytes below the melting temperature of PEO, the enhancement of ionic conductivity can be primarily related to decreased PEO crystallinity.

Another reason for this is because of the special conducting pathways provided by the PZSNT fillers. Since PZSNT is a porous inorganic–organic hybrid nanofiller, the interface between PZSNT and PEO matrix may act as a special conducting pathway for the charge carriers [30–35]. At high temperatures above the melting temperature of PEO, the increase of conductivity with PZSNT content is
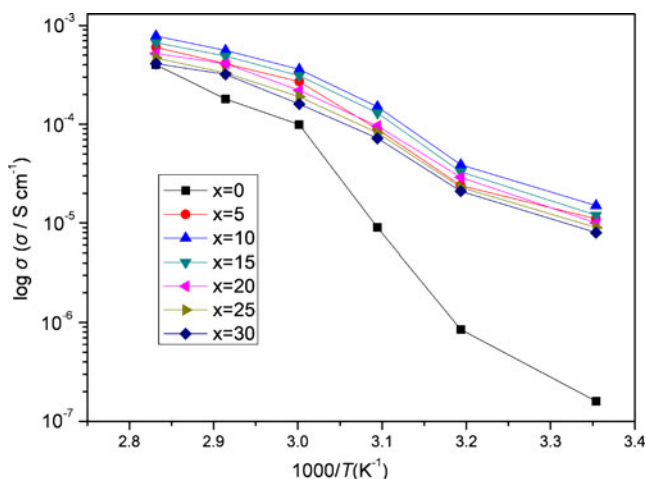

Fig. 3 Temperature dependence of ionic conductivity for PEO$_{10}$–LiClO$_4$/x% PZSNT composite polymer electrolytes
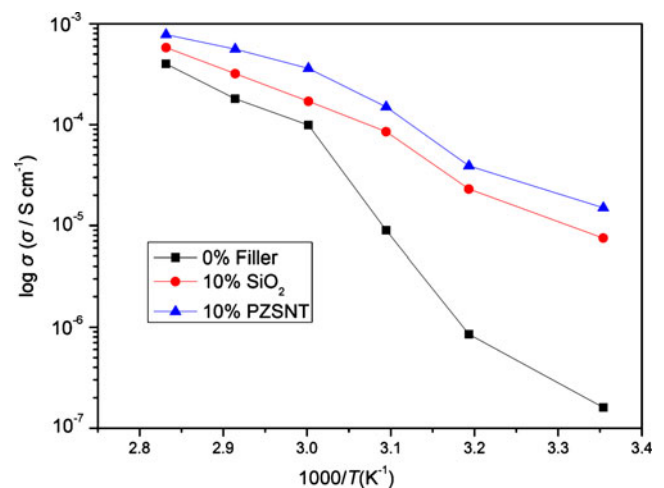

Fig. 4 Temperature dependence of ionic conductivity for PEO$_{10}$–LiClO$_4$, PEO$_{10}$–LiClO$_4$/10% SiO$_2$, and PEO$_{10}$–LiClO$_4$/10% PZSNT composite polymer electrolytes
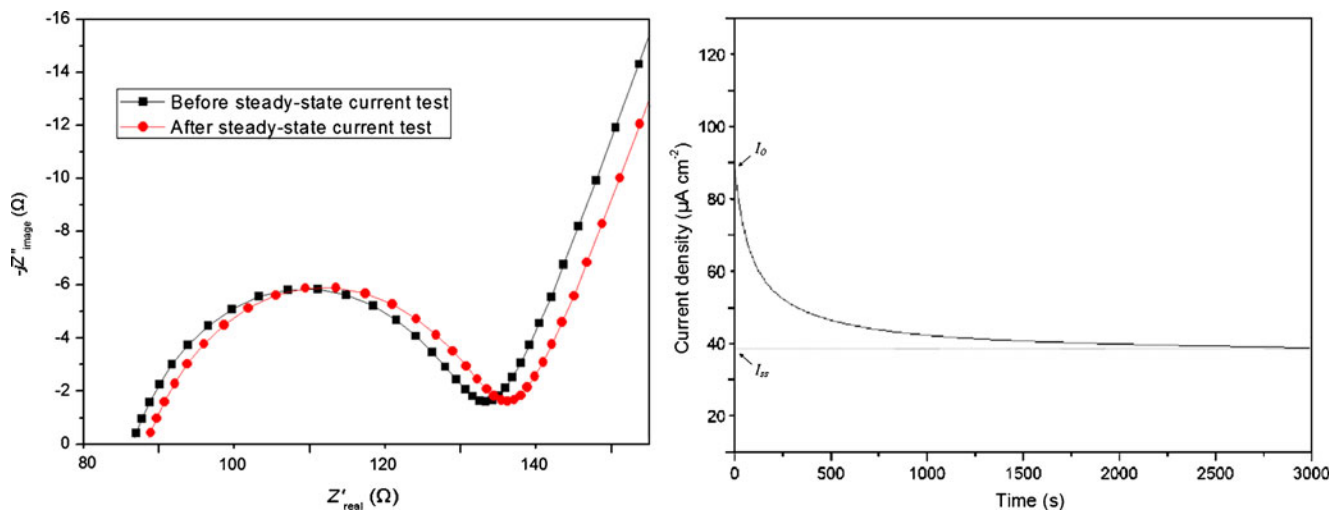
Fig. 5 ac and dc measurements for the lithium ion transference number of PEO_{10}–$LiClO_4$/10% PZSNT composite polymer electrolytes

basically due to the increasing amount of the special conducting pathways.

Figure 4 shows the conductivity of PEO_{10}–$LiClO_4$, PEO_{10}–$LiClO_4$/10% SiO_2 and PEO_{10}–$LiClO_4$/10% PZSNT at different temperatures. It can be seen that in the temperature range studied the conductivity of PEO_{10}–$LiClO_4$/10% PZSNT is higher than that of PEO_{10}–$LiClO_4$/10% SiO_2. The above reasoning may explain this result and show that compared with traditional ceramic fillers such as SiO_2, that PZSNT filler can enhance ionic conductivity more effectively.

Lithium ion transference number

The lithium ion transference number, T_{Li}^+, is very important in the development of rechargeable lithium ion batteries. A relatively high T_{Li}^+ can diminish the concentration gradients within the batteries and ensure proper battery operation at high current density. Figure 5 shows the ac and dc measurements of PEO_{10}–$LiClO_4$/10% PZSNT polymer electrolytes. T_{Li}^+ of PEO_{10}–$LiClO_4$ before and after the addition of PZSNT fillers are compared in Table 2, and it can be seen that T_{Li}^+ of the composite polymer electrolytes can be obviously increased by the addition of PZS nanotubes.

In the PEO_{10}–$LiClO_4$ complex, Li^+ can coordinate not only with the ether O in PEO chains but also with the O

atoms in ClO_4^-, but then its transport ability is restricted, resulting in a very low T_{Li}^+ value. After the addition of PZSNT, T_{Li}^+ can be increased. The O, N, and S atoms on the surface of PZSNT can interact with Li^+ and hence weaken the interactions between Li^+ and the O atoms of PEO chains and ClO_4^- and enhance the dissolvability of $LiClO_4$ to free more Li^+.

On the other hand, the interface between the inorganic–organic hybrid framework of PZSNT and PEO chains may provide a novel conducting pathway for Li^+ ions. The addition of PZSNT fillers could provide a highly conducting layer at the electrolyte/filler interface [30–35]. This interface layer may be an amorphous polymer layer surrounding PZSNT and a space-charge layer [36, 37]. The existence of the conductive layers between the inorganic–organic hybrid surface of PZSNT and PEO chains could act as the special conducting

Table 2 Lithium ion transference numbers of pristine PEO_{10}–$LiClO_4$ and PEO_{10}–$LiClO_4$/10% filler composite polymer electrolytes at 70 °C

Sample	PEO_{10}–$LiClO_4$	PEO_{10}–$LiClO_4$/ 10% SiO_2	PEO_{10}–$LiClO_4$/10% PZSNT
T_{Li+}	0.19	0.24	0.35
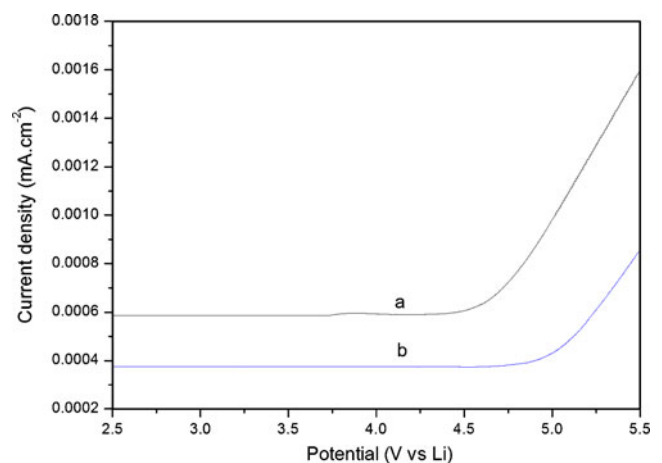
Fig. 6 Current–voltage responses of **a** PEO_{10}–$LiClO_4$ and **b** PEO_{10}–$LiClO_4$/10% PZSNT composite polymer electrolytes at 80 °C on a stainless steel working electrode at a scanning rate of 1 mV s^{-1}

pathway of the charge carriers and enhance the lithium ion transference number with the addition of PZSNT fillers.

Electrochemical stability window

The electrochemical stability window of polymer electrolytes can be obtained by the linear voltage sweep technique. Figure 6 displays the linear voltage sweep curves of pristine PEO_{10}–$LiClO_4$ and PEO_{10}–$LiClO_4$/10% PZSNT composite polymer electrolytes at 80 °C. The irreversible onset of the current determines the electrolyte breakdown voltage. The maximum working voltage (V_{max}) of PEO_{10}–$LiClO_4$ only extends to about 4.5 V versus Li, and the addition of PZSNT widens the electrochemical stability window. The V_{max} of PEO_{10}–$LiClO_4$/10% PZSNT exceeds to 4.9 V, indicating that PZSNT obviously improves the electrochemical stability. The good electrochemical stability suggested that this composite polymer electrolyte could be used as a candidate electrolyte material for rechargeable lithium polymer batteries whose working voltage is higher than 4.5 V.

Conclusions

In summary, novel PEO-based all solid-state composite polymer electrolytes using porous inorganic–organic hybrid PZS nanotubes as fillers have been fabricated. The PZS nanotubes serve as excellent fillers to polymer electrolytes because of their porous inorganic–organic hybrid structure. Compared with traditional ceramic fillers such as SiO_2, PZSNT is a more effective additive in PEO-based polymer electrolytes for enhancing their ionic conductivity. PZS nanotubes can also enhance other electrochemical properties, such as lithium ion transference number, and the electrochemical stability window of the composite polymer electrolytes. The optimum value of the PZS nanotube loading was found to be 10 wt.%. Their excellent electrochemical properties such as high room temperature ionic conductivity and lithium ion transference number combined with wide electrochemical stability window may ensure the use of PEO_{10}–$LiClO_4$/PZSNT composites as candidate electrolyte materials for solid-state rechargeable lithium polymer batteries.

References

1. Gray FM (1997) Polymer electrolytes. The Royal Society of Chemistry, Cambridge
2. Dias FB, Plomp L, Veldhuis JBJ (2000) J Power Sources 88:169–191
3. Croce F, Appetechi GB, Persi L, Scrosati B (1995) Nature 373:557–558
4. Croce F, Fiory FS, Persi L, Scrosati B (2001) Electrochem Solid State Lett 4:A121–A123
5. Kumar B, Scanlon LG (2000) J Electroceram 5:127–139
6. Kim J, Ji K, Lee J, Park J (2003) J Power Sources 119:415–421
7. Croce F, Appetecchi GB, Persi L, Scrosati B (1998) Nature 394:456–458
8. Yang YWC, Chen SY, Yuan CY, Yan DP (2005) Macromolecules 38:2710–2715
9. Wang ZX, Huang XJ, Chen LQ (2003) Electrochem Solid State Lett 6:E40–E44
10. Xiong HM, Zhao KK, Zhao X (2003) Solid State Ionics 159:89–95
11. Xi JY, Mao SJ, Tang XZ (2004) Macromolecules 37:8592–8598
12. Xi J, Qiu XP, Zhu WT (2006) Micropor Mesopor Mater 88:1–7
13. Nan CW, Fan LZ, Lin YH (2003) Phys Rev Lett 91:266104
14. Wieczorek W, Stevens JR, Florjanczyk Z (1996) Solid State Ionics 85:67–72
15. Croce F, Persi L, Scrosati B, Fiory FS, Plichta E, Hendrickson MA (2001) Electrochim Acta 46:2457–2461
16. Chung SH, Wang Y, Persi L, Croce F, Greenbaum SG, Scrosati B, Plichta E (2001) J Power Sources 97:644–648
17. Allcock HR (2004) Phosphorus Sulfur 179:661–671
18. Singh A, Krogman NR, Sethuraman S, Nair LS, Sturgeon JL, Brown PW, Laurencin CT, Allcock HR (2006) Biomacromolecules 7:914–918
19. Zhu L, Xu YY, Yuan WZ, Xi JY, Huang XB, Tang XZ, Zheng SX (2006) Adv Mater 18:2997–3000
20. Fu JW, Huang XB, Zhu L, Tang XZ (2008) Scr Mater 58:1047–1049
21. Jaeger RD, Gleria M (1998) Prog Polym Sci 23:179–276
22. Xi J, Qiu XP, Cui MZ, Tang XZ, Zhu WT, Chen LQ (2006) J Power Sources 156:581–588
23. Bruce PG, Vincent CA (1987) J Electroanal Chem 225:1–17
24. Evans J, Vincent CA, Bruce PG (1987) Polymer 28:2324–2328
25. Riley M, Fedkiw PS, Khan SA (2002) J Electrochem Soc 149:A667–A674
26. Heitner KL (2000) J Power Sources 89:128–131
27. Luther TA, Stewart F, Budzien JL, LaViolette RA, Bauer WF, Harrup MK, Allen CW, Elayan A (2003) J Phys Chem 107:3168–3176
28. Li X, Hsu SL (1984) J Poly Sci Polym Phys Ed 22:1331–1342
29. Kim S, Park SJ (2007) Electrochim Acta 52:3477–3484
30. Gray FM (1991) Solid polymer electrolytes—fundamentals and technical applications. VCH, Wenheim
31. Salomon M, Xu M, Eyring EM, Petrucci S (1994) J Phys Chem 98:8234–8244
32. Nan CW, Smith DM (1991) Mater Sci Eng B 10:99–106
33. Nan CW (1993) Prog Mater Sci 37:1–116
34. Wieczorek W, Raducha D, Zalewska A (1998) J Phys Chem B 102:8725–8731
35. Wieczorek W, Zalewska A, Raducha D, Florjanczyk Z, Stevens JR (1996) Macromolecules 29:143–155
36. Maier J (1995) Prog Solid State Chem 23:171–263
37. Sata N, Eberman K, Eberl K, Maier J (2000) Nature 408:946–949